Int. J. Solids Structures, 1967, Vol. 3, pp. 543 to 564. Pergamon Press Ltd. Printed in Great Britain

AN ANALYTIC METHOD FOR ELASTIC–PLASTIC SOLUTIONS

I. S. TUBA

Mechanics Department, Westinghouse Research Laboratories, Pittsburgh, Pennsylvania

Abstract—The general three dimensional elastic–plastic problem is formulated in terms of the total displacements and the plastic strain components. The resulting governing equations are applicable to arbitrary orthogonal curvilinear coordinate systems and to arbitrary theories of plasticity. A method is developed for the solution of two dimensional problems, and it is used for the analysis of a circular hole in a flat plate under uniaxial tension. The same method could be generalized for three dimensions.

The purpose of the paper is to illustrate that a straightforward, simple approach can be used to formulate and solve otherwise very complicated and mostly unsolved elastic–plastic problems.

NOTATION

ϵ_{ij}	total strain components
ϵ'_{ij}	elastic strain components
ϵ''_{ij}	plastic strain components
τ_{ij}	stress components
u_i, u, v, w	displacement components
E	modulus of elasticity
ν	Poisson's ratio
$\lambda = \dfrac{E\nu}{(1+\nu)(1-2\nu)}$, $\mu = \dfrac{E}{2(1+\nu)}$	Lamé constants
α	coefficient of thermal expansion
β	$\alpha(3\lambda+2\mu)$
T	temperature
δ_{ij}	Kronecker delta
Θ	strain invariant
F_i	component of body force
ρ	density of material
f	loading function, yield condition or yield function
C	a scalar which may depend on stress, strain and their history
g_{ij}	metric coefficients
h_i	distortion coefficients
x_1, x_2, x_3	curvilinear coordinates
$C_{i;j}$	variable coefficient of $\partial u_i/\partial x^j$ term in the differential equation
$\varkappa_i, b_i$	constants defined in the Appendix
ω	over-relaxation factor
σ_Y	yield strength of an actual stress–strain curve when set equal to the proportional limit
σ_0	yield strength for bilinear representation of stress–strain curves (see Fig. 2)

For a, r_∞, m, n, M, N, r_m, dr_m, $d\theta$, θ_n see Fig. B1.

K_σ, K_ϵ	stress and strain concentration factors

1. INTRODUCTION

PLANE elastic–plastic problems have been formulated in terms of an elastic–plastic stress function and the plastic strains by the writer [1,2]. Similar formulations have been considered also by Roberts and Mendelson [3] for thermal stress problems. The method is very convenient for the solution of plane, singly connected regions. It can also be used for multiply connected regions but the determination of the linear part of the elastic–plastic stress function becomes quite complicated.

The purpose of the present paper is to formulate three dimensional and plane problems in terms of the total displacements and plastic strain components. Solutions will have the same degree of complexity for singly or doubly connected regions.

A method of solution of the governing equations is illustrated on the problem of a circular hole in a unidirectionally stressed flat plate. It is believed that the same method can be used also for the solution of some three dimensional problems.

2. FORMULATION OF GOVERNING RELATIONS

For convenience the general three dimensional problem is discussed with the use of tensor notations.

Consider the following basic equations:

Strain–displacement relations

$$\epsilon_{ij} = \tfrac{1}{2}(u_{i,j}+u_{j,i}) = \epsilon'_{ij}+\epsilon''_{ij} \tag{1}$$

Elastic stress–strain relations

$$\tau_{ij} = \lambda g_{ij}\Theta' + 2\mu\epsilon'_{ij} - \beta T g_{ij} \tag{2}$$

where

$$\Theta' = g^{ij}\epsilon'_{ij} = \epsilon'^{i}_{i} \tag{3}$$

Equilibrium equations

$$g^{jk}\tau_{ij,k} + F_i = \rho\ddot{u}_i \tag{4}$$

Substitute equation (2) into equation (4)

$$g^{jk}\left(\lambda g_{ij}\frac{\partial\Theta'}{\partial x^k} + 2\mu\epsilon'_{ij,k} - \beta g_{ij}\frac{\partial T}{\partial x^k}\right) + F_i = \rho\ddot{u}_i \tag{5}$$

or

$$\lambda\frac{\partial\Theta'}{\partial x^i} + 2\mu g^{jk}\epsilon'_{ij,k} - \beta\frac{\partial T}{\partial x^i} + F_i = \rho\ddot{u}_i. \tag{6}$$

But from equation (1)

$$g^{jk}\epsilon'_{ij,k} = \frac{1}{2}g^{jk}(u_{i,jk}+u_{j,ik}) - g^{jk}\epsilon''_{ij,k}$$

$$= \frac{1}{2}g^{jk}u_{i,jk} + \frac{1}{2}\frac{\partial\Theta}{\partial x^i} - g^{jk}\epsilon''_{ij,k}. \tag{7}$$

Since

$$g^{jk}u_{j,ik} = u^k{}_{,ki} \quad \text{and} \quad u^k{}_{,k} = \Theta. \tag{8}$$

Note that because of the incompressibility of the plastic part of the material $\Theta'' = 0$, therefore

$$\Theta' = \Theta. \tag{9}$$

Substitute equation (7) into equation (6)

$$(\lambda+\mu)\frac{\partial\Theta}{\partial x^i}+\mu g^{jk}u_{i,jk}-2\mu g^{jk}\epsilon''_{ij,k}-\beta\frac{\partial T}{\partial x^i}+F_i = \rho\ddot{u}_i. \tag{10}$$

But

$$g^{jk}u_{i,jk} = \nabla^2 u_i,$$

therefore

$$(\lambda+\mu)\frac{\partial\Theta}{\partial x^i}+\mu\nabla^2 u_i = \rho\ddot{u}_i-F_i+\beta\frac{\partial T}{\partial x^i}+2\mu g^{jk}\epsilon''_{ij,k}. \tag{11}$$

The governing relation as given in equation (11) must be accompanied by the initial and boundary conditions. It should be noted that for continuous and singly valued displacements, the conditions of compatibility are automatically satisfied.

Plastic strain components depend on the past history of the deformation

$$\epsilon''_{ij} = \int_{\mathrm{LP}} \mathrm{d}\epsilon''_{ij} \tag{12}$$

where

$$\begin{aligned} \mathrm{d}\epsilon''_{ij} &= C\frac{\partial f}{\partial \tau_{ij}}\cdot\frac{\partial f}{\partial \tau_{kl}}\mathrm{d}\tau_{kl} && \text{when loading} \\ \mathrm{d}\epsilon''_{ij} &= 0 && \text{when unloading} \end{aligned} \tag{13}$$

and LP indicates loading path.

References [1–3] discuss the methods of computing plastic strain components. The methods are not discussed in the present paper in detail. Expression (11) is a tensor equation. Since our prime interest is elastic–plastic stress and strain concentration it is necessary to expand equation (11) for various orthogonal curvilinear coordinates. The results are given in the appendix for the general case in terms of the distortion coefficients. Inertia and body forces are not included and uniform temperature is assumed. As an example, a polar coordinate system is considered.

For equilibrium in the r direction let $x_1 = r$, $x_2 = \theta$, $u_1 = u$, $u_2 = v$, $h_1 = 1$ and $h_2 = r$ in equations (A1) and (A3) of the Appendix.

For equilibrium in the θ direction take $x_1 = \theta$, $x_2 = r$, $u_1 = v$, $u_2 = u$, $h_1 = r$ and $h_2 = 1$. After some rearrangements the following two equations are obtained

$$\begin{aligned} \frac{\partial}{\partial r}\left[\frac{1}{r}\frac{\partial}{\partial r}(ru)\right]+\frac{\partial}{\partial\theta}\left[\frac{1-\nu}{2r^2}\frac{\partial u}{\partial\theta}-\frac{3-\nu}{2}\frac{v}{r^2}+\frac{1+\nu}{2r}\frac{\partial v}{\partial r}\right] &= \frac{\partial\epsilon''_r}{\partial r}+\frac{1-\nu}{r}\epsilon''_r+\nu\frac{\partial\epsilon''_\theta}{\partial r} \\ &\quad -\frac{1-\nu}{r}\epsilon''_\theta+\frac{1-\nu}{2r}\frac{\partial\gamma''_{r\theta}}{\partial\theta} \end{aligned} \tag{14a}$$

$$\frac{1-\nu}{2}\frac{\partial}{\partial r}\left[\frac{1}{r}\frac{\partial}{\partial r}(rv)\right]+\frac{\partial}{\partial \theta}\left[\frac{3-\nu}{2}\frac{u}{r^2}+\frac{1+\nu}{2r}\frac{\partial u}{\partial r}+\frac{1}{r^2}\frac{\partial v}{\partial \theta}\right]=\frac{\nu}{r}\frac{\partial \epsilon_r''}{\partial \theta}+\frac{1}{r}\frac{\partial \epsilon_\theta''}{\partial \theta}+\frac{1-\nu}{2}\frac{\partial \gamma_{r\theta}''}{\partial r}+\frac{1-\nu}{r}\gamma_{r\theta}''. \tag{14b}$$

Of course these equations could be derived in polar coordinates without the use of equation (A1), but a corresponding development for other coordinate systems could be very involved by a direct formulation.

3. EXAMPLE: CIRCULAR HOLE IN A UNIDIRECTIONALLY STRESSED FLAT PLATE

A flat plate of infinite extension is considered which is stretched in the x direction by a known one directional stress σ_∞ at infinity. A circular hole is located in the plate with its center placed at the origin. It is convenient to use the polar coordinate system shown in Fig. 1. The loading is such that the portion of the plate around the hole is stressed beyond

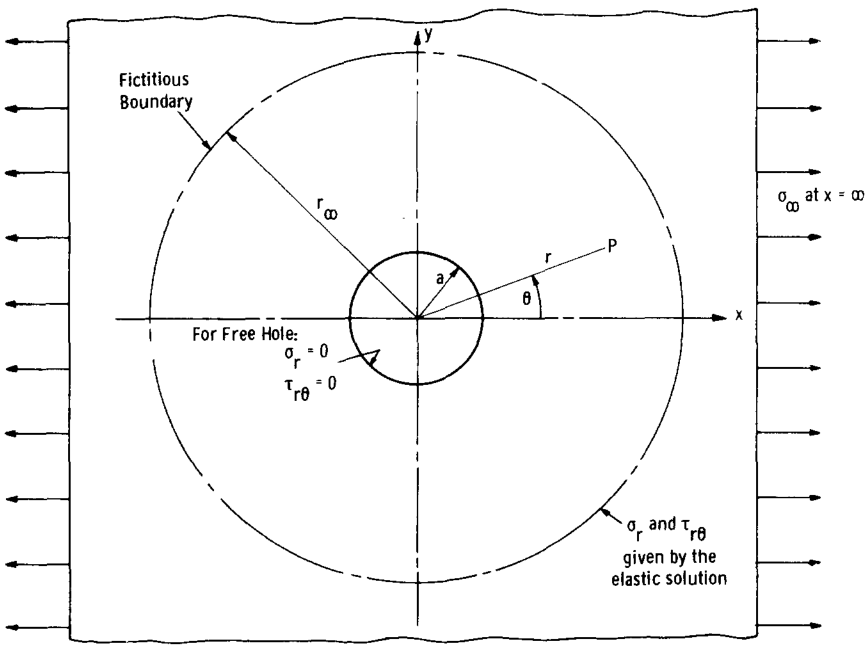

FIG. 1. Illustration of the geometry.

the elastic limit of the material. The usual plane stress assumptions are used. The elastic solution [4] to this problem is well known and will not be repeated here. It is only noted that the maximum tangential stress and strain concentration factors are at $r = a$ and $\theta = \pm\pi/2$

$$K_\sigma = \frac{\sigma_\theta}{\sigma_\infty} = K_\epsilon = \frac{\epsilon_\theta}{\epsilon_{\theta,\infty}} = 3. \tag{15}$$

The effective stress and strain concentration factors are also equal to three.

Review of previous work

Since in [1] of this paper the writer reviewed in detail the recent state of both theoretical and experimental elastic–plastic analysis, here only a brief account is given for the example in consideration.

Stowell [7] formulated the problem in terms of the secant modulus. Approximate stress distribution was adjusted to minimize the mean square of the error in satisfying the equilibrium equations. There were no considerations given to compatibility of strains. Although Stowell's procedure is questionable in several respects, it is still commendable for two reasons: It is the first attempt known to the writer to solve a two dimensional elastic–plastic problem for arbitrary stress–strain curves; furthermore it is simple to use by a trial and error method.

The work of Budiansky and Vidensek [8] is considerably more sophisticated. The solution for the final stress components is obtained by adding a corrective solution to the elastic solution of the corresponding problem. The stress–strain curve used is that of Ramberg and Osgood [9]. The solution is based on the simple deformation theory of plasticity and is found by application of a variational principle in conjunction with the Rayleigh–Ritz procedure.

The formulation is very lengthy and involved. The approximate solution is possible by computers using numerical techniques. The method of Budiansky and Vidensek could be applied to other geometries but as presented in [8] it is applicable only to the circular hole problem. For small loads and low strain hardening the results agree fairly well with the results of Stowell, but for high loads and considerable strain hardening the disagreement is pronounced.

Griffith [10] experimentally investigated the case of a circular hole in flat 24S-T aluminum panels using electromagnetic strain gages.

The same material was used by Box [11] but the strain measurements were made by measuring the distance between gage marks with an optical slide comparator which read directly to 0·00005 of an inch.

A photoelastic coating technique was used by Dixon [12] on flat aluminum bars.

An experimental determination of the elastic–plastic stress and strain distribution by the Moiré method is given by Durelli and Sciammarella [13].

Fried and Shoup [14] found that the photoelastic effect in polyethylene varies linearly with principal strain difference well beyond the range of stress–strain linearity for this material. The nondimensional stress–strain curve for polyethylene over the range of strain rates employed was found to be similar to that of 3.S aluminum.

Frocht and Thomson [15] used thin models of cellulose nitrate to extend the photoelastic method to the plastic state.

A quantitative comparison of the results of these investigations seems very difficult if not impossible because of the numerous variables involved.

Since the stress–strain curves of Theocaris and Marketos [5] and Johnson [6] are used in the present work, some of their results will be reported in Section 5.

This brief review is concluded with the appropriate remark of Budiansky and Vidensek [8]: "The theoretical solution presented for the stresses in the plastic range around a circular hole in a plate subjected to uniaxial tension is very far from a final answer to the problem considered."

The present paper cannot offer that final answer either. On the other hand it presents a very simple formulation readily applied to a wide variety of geometries and either to the deformation or to the incremental theories of plasticity.

Method of solution

Consider equations (14) written in a symbolic form as

$$D_{11}u+D_{12}v = \Phi \tag{16a}$$

$$D_{21}u+D_{22}v = \Psi \tag{16b}$$

where the D's are the given differential operators, and Φ and Ψ represent the right sides.

The elastic solution, given in [4], satisfies equations (16) if $\Phi = \Psi = 0$. This solution can be denoted by $u_{0,0}$ and $v_{0,0}$. In what follows the first subscript of u and v will denote how many times the right sides have been reestimated and the second subscript the number of iterations applied to the displacement components for a given estimate of the right side. From this elastic solution, which will contain stresses above the elastic limit, the elastic–plastic problem is attacked by the procedure described in the next paragraph.

From the elastic solution estimate an initial value of the plastic strain components by subtracting the elastic strains from the total strains derived from $u_{0,0}$ and $v_{0,0}$. The procedure for doing this is given in [1–3].

Compute the corresponding right sides and denote them by Φ_0 and Ψ_0. Closed form solution of this problem seems impossible, but the equations can be put into finite difference form and solved by relaxation or other techniques. For example, equations (16) can be solved by the following iteration sequence:

$$D_{11}u_{1,i} = \Phi_0 - D_{12}v_{1,i-1} \tag{17a}$$

$$D_{22}v_{1,i} = \Psi_0 - D_{21}u_{1,i}. \tag{17b}$$

The iteration can be stopped when the solution stabilizes. Based on the new solution the right sides are recomputed and the sequence is repeated until the plastic strains stabilize. For the pth iteration on the plastic strains and the ith iteration on the displacement, equations (16) take the form

$$D_{11}u_{p,i} = \Phi_{p-1} - D_{12}v_{p,i-1} \tag{18a}$$

$$D_{22}v_{p,i} = \Psi_{p-1} - D_{21}u_{p,i}. \tag{18b}$$

The above outlined method can be adopted equally well for the total or deformation theories and for the incremental theories of plasticity, and can be used for arbitrary non-linear strain hardening materials including the elastic perfectly plastic condition as a limiting case. It is postulated that there is a relationship between the effective stress and the effective plastic strain which, in general, need not be an explicit function, but for practical reasons in most cases, it is displayed in the form of the usual stress–strain curves.

An alternate to the sequence of iterations given by equations (18) can be performed as follows: Continuously compare the relative residuals of the two equations to each other, and resolve the one which has the larger relative residual. Relative residuals are defined as the ratio of the maximum present residual to the maximum residual for the exact elastic solution.

In numerical solutions infinite regions cannot be used. Instead an outer boundary with a large radius is considered. Radial and shear stresses are maintained on this boundary which are the same as given by the corresponding elastic solution for that circle. Of course the displacements could be specified at the boundaries instead of the load just as well.

Because of symmetry only one fourth of the region is used.

From equations (1) and (2) the following conditions are obtained:

At $r = a$ and $r = r_\infty$

$$\left.\frac{\partial u}{\partial r}\right|_{p,i} = \frac{\sigma_r^0(1-\nu^2)}{E} - \frac{\nu}{r}\left[u + \frac{\partial v}{\partial \theta}\right]_{p,i-1} + \left[\epsilon_r'' + \nu\epsilon_\theta''\right]_{p-1} \tag{19a}$$

$$\left.\frac{\partial v}{\partial r}\right|_{p,i} = \frac{\tau_{r\theta}^0}{G} + \frac{1}{r}\left[v - \frac{\partial u}{\partial \theta}\right]_{p,i} + \left.\gamma_{r\theta}''\right|_{p-1}. \tag{19b}$$

At $\theta = 0$ and $\theta = \frac{\pi}{2}$

$$v_{p,i} = 0 \tag{19c}$$

$$\left.\frac{\partial u}{\partial \theta}\right|_{p,i} = 0. \tag{19d}$$

These conditions are sufficient for the solution of the problem.

Establishment of the quantities Φ and Ψ near the elastic–plastic boundary requires special attention in certain cases. The governing equations (14) apply equally well for the elastic region where the right side is zero, and for the plastic region where the right side depends on the plastic strains. For many real materials, elastic–plastic boundaries are very difficult to define because the transition is very smooth. On the other hand when an idealized material is assumed, with well defined yield point, there are discontinuities in the derivatives of the stresses and plastic strains at the elastic–plastic interface. Fortunately this causes no more difficulty in the computations than a real boundary. Simply, when derivatives are evaluated the appropriate forward or backward difference equations are used.

The writer cannot offer proof of uniqueness of the solution. In any problems considered the resulting displacements were continuous.

Since the above description of the method of solution is very symbolic a somewhat more detailed discussion on a numerical method of solution is presented in Appendix B.

4. DISCUSSION OF RESULTS

The method of solution as described in the previous section, and in the Appendix, provides the stress, strain and displacement components at every node point of a curvilinear network. Due to space limitations it is not possible to give these data. The following is restricted mostly to the illustrations of the development of the elastic–plastic boundaries and of the maximum stress and strain concentration factors. In the calculations which have been performed by the present method, actual stress–strain curves have been used. These stress–strain curves were taken from such references which already consider some form of analysis for the circular hole problem.

There are no experimental results available which correspond exactly to the infinite plate assumptions. Some experimental results have been published for perforated strips, therefore the comparison which follows will be more qualitative than quantitative.

In the examples, a circular hole of unit radius is considered.

Although it is known that incremental theories give more realistic solutions the present examples are worked out for a deformation theory based on the von Mises flow criteria. The method is applicable to both theories but the deformation theory requires less work than the incremental theory.

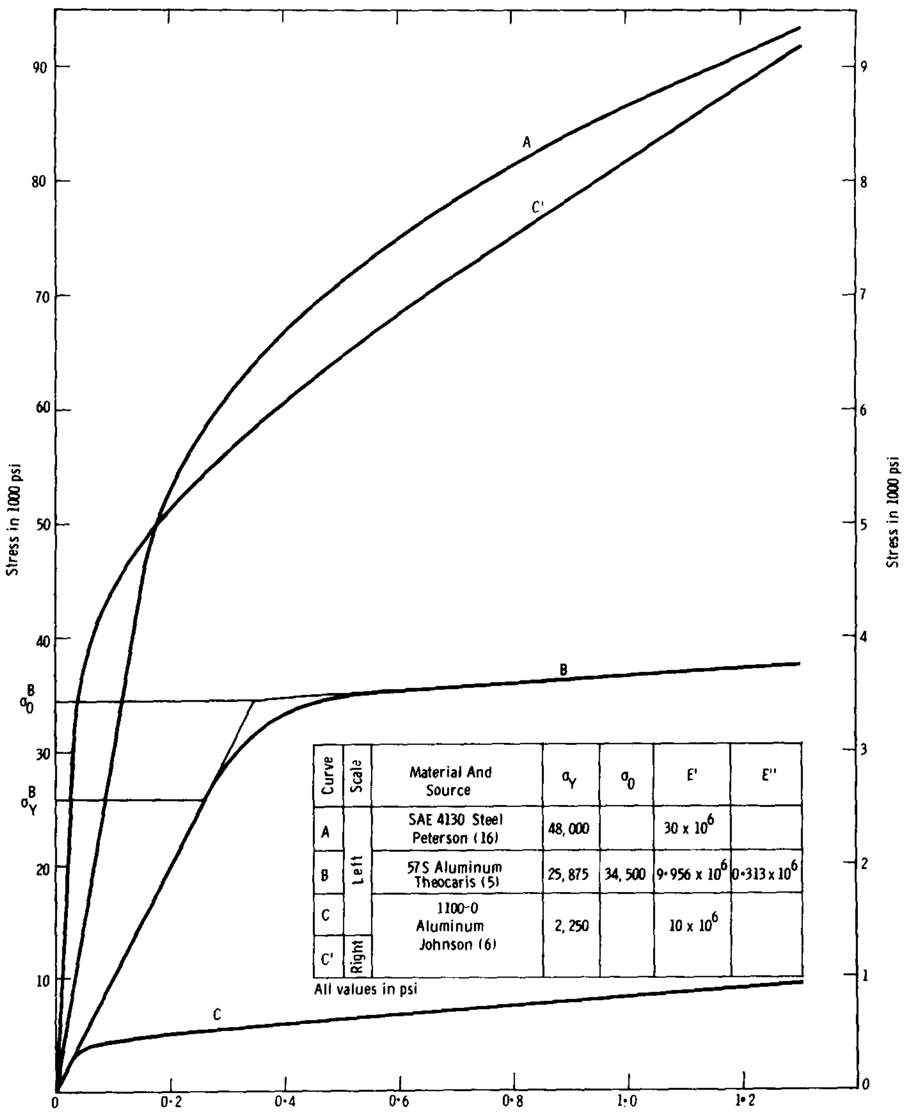

Curve	Scale	Material And Source	σ_Y	σ_0	E'	E''
A	Left	SAE 4130 Steel Peterson (16)	48,000		30 x 10^6	
B	Left	57S Aluminum Theocaris (5)	25,875	34,500	9·956 x 10^6	0·313 x 10^6
C	Left	1100-0 Aluminum Johnson (6)	2,250		10 x 10^6	
C'	Right	(as C)				

All values in psi

FIG. 2. Uniaxial stress–strain curves.

The maximum stress and strain concentration factors, in each case discussed, apply to the points $r = a$, $\theta = \pm\frac{\pi}{2}$, and they are defined as

$$K_{\sigma_\theta} = \frac{\sigma_\theta}{\sigma_{\theta_\infty}} = K_{\sigma_e} = \frac{\sigma_{\text{eff}}}{\sigma_{\text{eff},\infty}}, \tag{20a}$$

$$K_{\epsilon_\theta} = \frac{\epsilon_\theta}{\epsilon_{\theta_\infty}} \quad \text{and} \quad K_{\epsilon_e} = \frac{\epsilon_{\text{eff}}}{\epsilon_{\text{eff},\infty}}. \tag{20b}$$

Normalized steel

Peterson [16] applied Stowel's [7] method to the stress–strain curve of SAE 4130 normalized steel (see curve A of Fig. 2). Stowel's method produces the concentration factors which are shown by the dashed lines on Fig. 3.

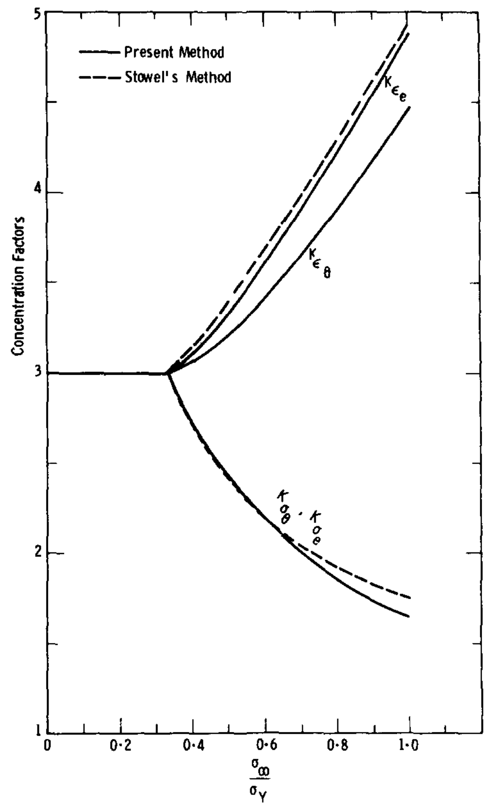

FIG. 3. Comparison of stress and strain concentration factors for SAE 4130 annealed steel for Stowel's and the present method.

The same stress–strain curve has been used also by the writer in the present study. The resulting concentration factors are shown by the solid lines in Fig. 3. Since at $r = a$; $\theta = \pm\pi/2$ the only stress component is σ_θ, the effective and tangential stress concentration factors are the same. At the same point in addition to the tangential strain there also exists a radial strain, therefore the tangential and the effective strain concentration factors have different values. The shape of the elastic–plastic boundaries are shown on Fig. 4, for several stages of loading.

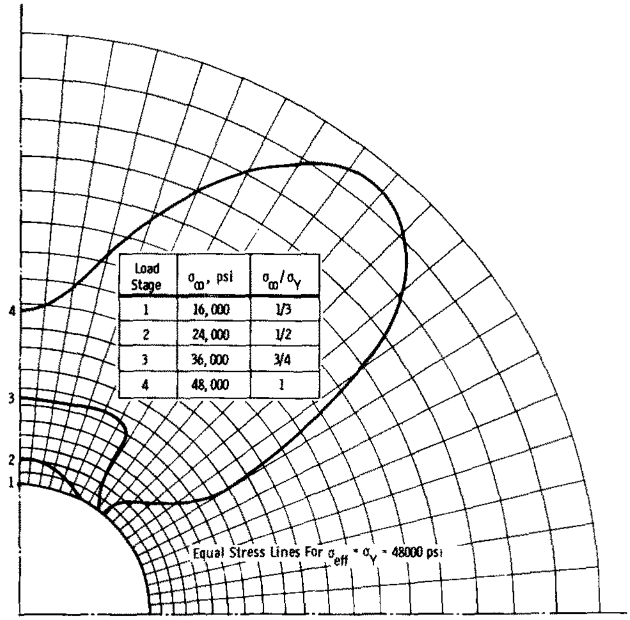

FIG. 4. Elastic–plastic boundaries for SAE 4130 normalized steel.

Aluminum alloy

Theocaris and Marketos [5] have used AA5357 (57S) aluminum alloy (curve B of Fig. 2) in their study of narrow perforated strips applying the birefringent coating method. The largest width to hole diameter ratio they used was three. Both the elastic and the elastic–plastic stress and strain concentration factors have two different values depending on what is used for the basis of comparison. The results of Theocaris and Marketos are shown in Fig. 5, with dashed lines. Following the notation of Theocaris and Marketos the subscript η refers to the case when the whole width of the strip is used for basis of comparison and subscript μ to the case when the comparison is based on the minimum cross section. The equal effective stress lines which correspond to $\sigma_{eff} = \sigma_0$ of the Theocaris–Marketos solution are given on Fig. 6. These lines would correspond to the elastic–plastic boundaries if the stress–strain curve would be approximated by the bilinear curve as shown in Fig. 2.

The actual stress–strain curve of Theocaris and Marketos was also used by the writer in the solution of the infinite plate problem. The resulting concentration factors are plotted in Fig. 7, and also in Fig. 5 with solid lines.

On Fig. 8 two sets of equal stress lines are shown, both of which are the results of the present solution. The dashed lines are for $\sigma_{eff} = \sigma_0$. These could be considered as elastic–plastic boundaries for a bilinear representation of the stress–strain curve. The other set, with solid lines, represent $\sigma_{eff} = \sigma_Y$, where σ_Y is the highest stress still on the linear part of the actual stress–strain curve. Since the results of Theocaris and Marketos apply to

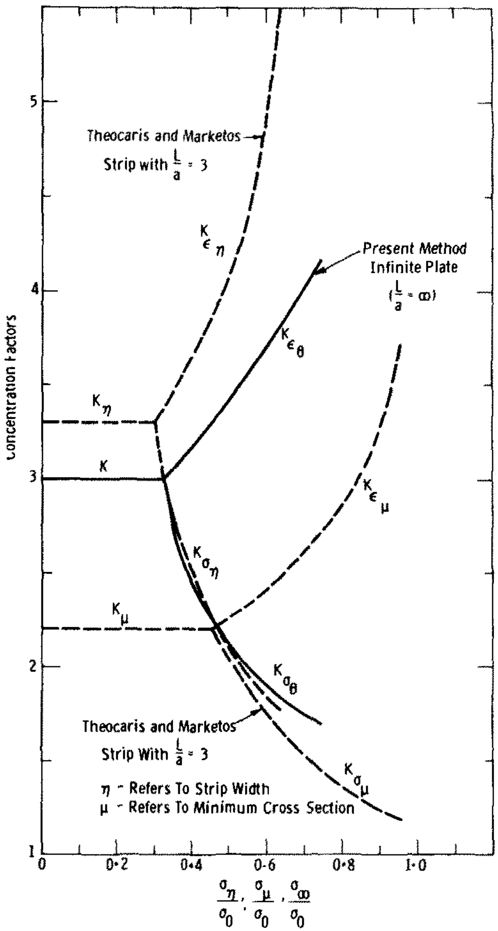

FIG. 5. Comparison of stress and strain concentration factors around a circular hole in a narrow strip (experimental, Theocaris and Marketos) and in an infinite plate (theoretical, present method) both for AA5357 (57S) aluminum alloy.

Load Stage	σ_η, psi	σ_η/σ_0 *	σ_μ, psi	σ_μ/σ_0 *
I	9,660	0·28	14,490	0·42
II	11,040	0·32	16,560	0·48
III	13,110	0·38	19,665	0·57
IV	15,525	0·45	23,288	0·675
V	17,595	0·51	26,393	0·765
VI	20,010	0·58	30,015	0·87
VII	21,735	0·63	32,603	0·945

Note * Values were estimated from the figures of Ref. 5

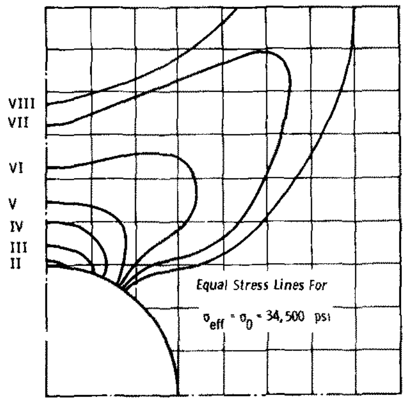

FIG. 6. Experimental results of Theocaris and Marketos for a strip with $L/a = 3$ [5].

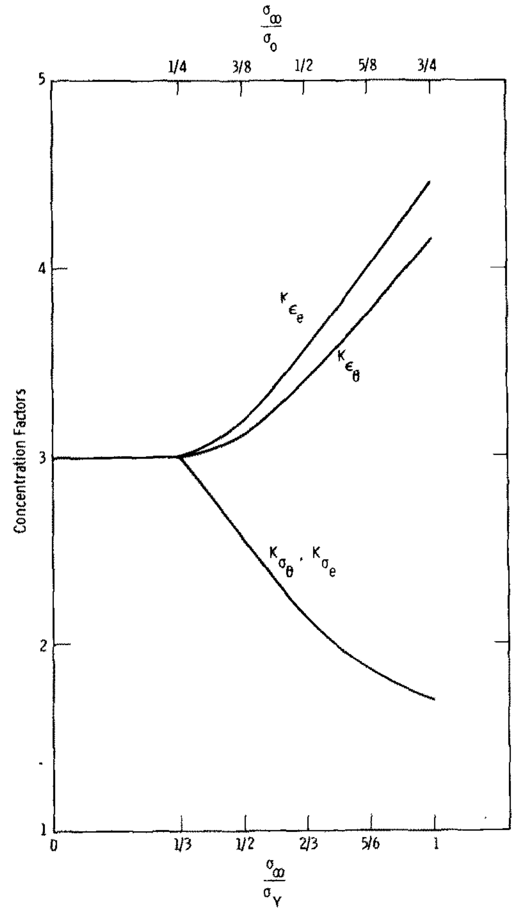

FIG. 7. Stress and strain concentration factors for AA5357 (57S) aluminum alloy.

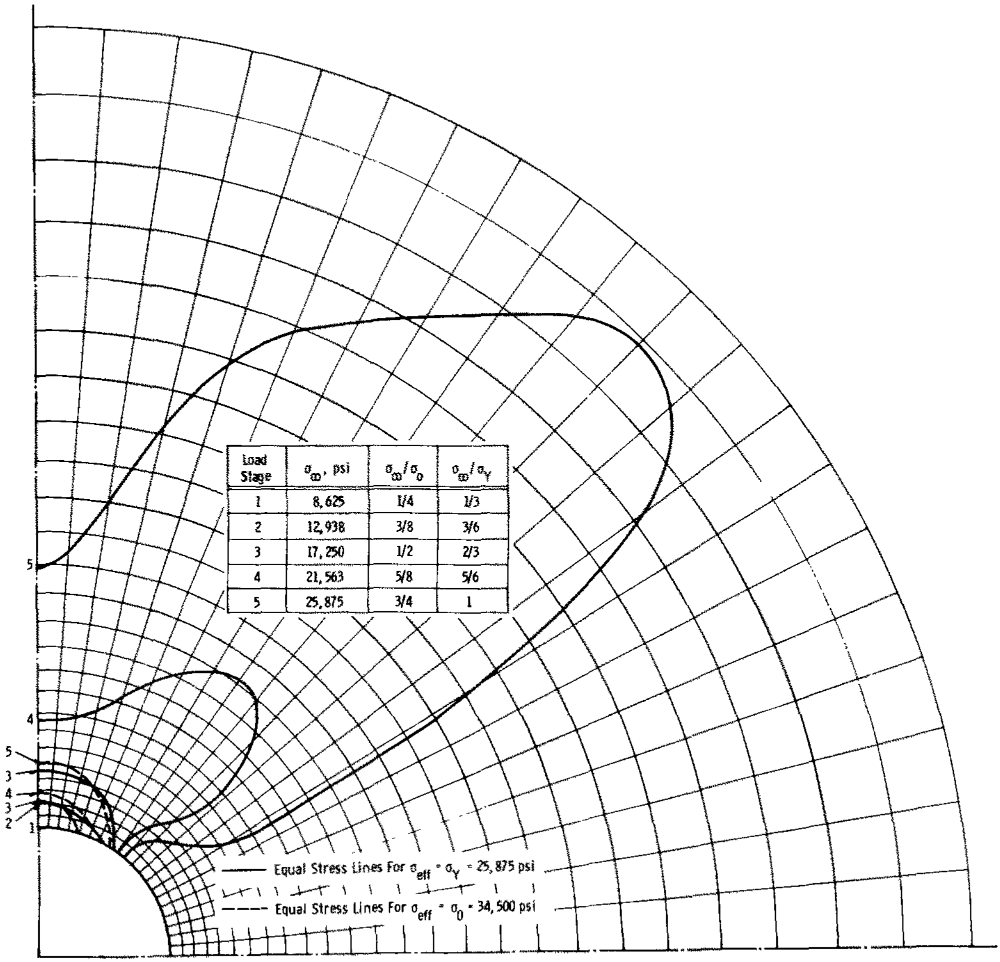

Load Stage	σ_∞, psi	σ_∞/σ_0	σ_∞/σ_Y
1	8,625	1/4	1/3
2	12,938	3/8	3/6
3	17,250	1/2	2/3
4	21,563	5/8	5/6
5	25,875	3/4	1

FIG. 8. Elastic–plastic boundaries for aluminum alloy AA5357 (57S).

the narrow strip and the present solution is for an infinite plate, any comparison of the two must be qualitative only. Due to the different nature of these problems it was not possible to use a common loading factor, therefore the loading stages do not correspond. It is important to note that the shape and size of the plastic region in the initial stages of yielding depend a great deal on the assumptions made concerning the transition part of the stress–strain curve.

Annealed aluminum

Johnson [6] used AA 1100 commercially pure annealed aluminum for perforated tensile panel specimen. The panel width to hole diameter ratio was six. The stress–strain curve of the material is plotted on Fig. 2, using two different scales. The scale on left should be used for curve C and the scale on the right for curve C′.

Johnson used strain gages to measure the strain along the minimum cross section. The actual stress–strain curve of Johnson has been used by the writer for the infinite plate and a comparison of results is carried out in Fig. 9. Since the load σ_∞ of the infinite plate cannot be compared directly either to the applied load σ_L, or to the average stress σ_A, both of these are indicated on the figure. Actually σ_∞ should correspond to some stress between σ_L and σ_A. The obtained results agree fairly well if we consider σ_A close to σ_∞. This can be justified on the basis that the strip is wide as compared to the diameter of the hole.

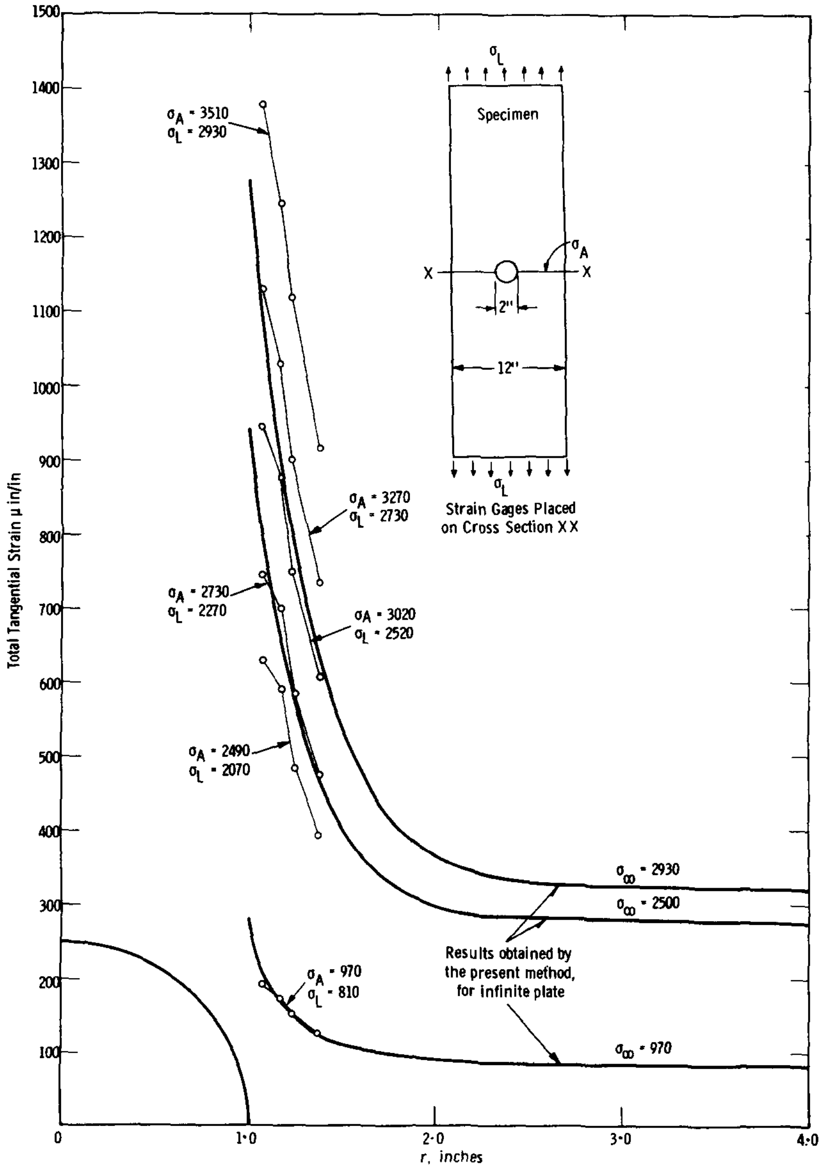

FIG. 9. Comparison of tangential total strains to Johnson's experimental results [6].

Whether any quantitative comparisons would be justified or not, based on the above results, it can be concluded that the analytical solutions as obtained by the method presented here are reasonable.

5. CONCLUSIONS AND GENERALIZATION

Elastic–plastic problems are formulated in terms of the displacements and the plastic strain components. The equations are given in terms of arbitrary orthogonal curvilinear coordinates for three dimensional, plane strain and plane stress conditions.

The formulation can be used for plane singly connected regions. Its advantage is more outstanding for multiply connected regions where the nonhomogeneous biharmonic equation method in terms of an elastic–plastic stress function leads to complications.

The present formulation can be used equally well both with the deformation theories and with the incremental theories of plasticity for arbitrary nonlinear stress–strain relations. Deformation theories require less work, but the incremental theories yield more accurate results.

The practicality of the formulation is illustrated for the problem of a circular hole in a unidirectionally stressed flat plate. An iterative method is presented for the solution of the two simultaneous second order nonhomogeneous partial differential equations.

It is noted that the same method can be generalized for three dimensional problems.

For three dimensional case, equation (A1) can be rewritten as

$$D_{11}u+D_{12}v+D_{13}w = \Phi \tag{21a}$$

$$D_{21}u+D_{22}v+D_{23}w = \Psi \tag{21b}$$

$$D_{31}u+D_{32}v+D_{33}w = \Omega \tag{21c}$$

A generalization of the method successfully used on the corresponding two dimensional problem (equations 10) would be the following double iterative procedure (see equations 18)

$$D_{11}u_{p,i} = \Phi_{p-1}-D_{12}v_{p,i-1}-D_{13}w_{p,i-1} \tag{22a}$$

$$D_{22}v_{p,i} = \Psi_{p-1}-D_{21}u_{p,i}-D_{23}w_{p,i-1} \tag{22b}$$

$$D_{33}w_{p,i} = \Omega_{p-1}-D_{31}u_{p,i}-D_{32}v_{p,i}. \tag{22c}$$

It is the intention of the writer to pursue the present approach for three dimensional problems in the future and possibly include the effects of large deformations.

Acknowledgement—Comments of Mr. Evan A. Davis are greatly appreciated.

REFERENCES

[1] I. S. TUBA, Elastic–plastic stress and strain concentration. Dissertation for the degree of Doctor of Philosophy, University of Pittsburgh (1964).
[2] I. S. TUBA, A method of elastic–plastic plane stress and strain analysis. *J. Strain Analysis* (Jan. 1966).
[3] E. ROBERTS and A. MENDELSON, Analysis of plastic thermal stresses and strains in finite thin plate of strain-hardening material. *NASA* TN-D-2206 (Oct. 1964).
[4] S. TIMOSHENKO and J. N. GOODIER, *Theory of Elasticity*, p. 78. McGraw-Hill (1951).
[5] P. S. THEOCARIS and E. MARKETOS, Elastic–plastic analysis of perforated thin strips of a strain hardening material. *J. Mech. Phys. Solids* **12**, 377 (1964).

[6] R. L. JOHNSON, Strain concentration around a circular hole in a soft aluminum sheet. Master of Science Thesis, University of Pittsburgh (1961).
[7] E. Z. STOWELL, Stress and strain concentration at a circular hole in an infinite plate. *National Advisory Committee for Aeronautics*, Technical Note No. 2073.
[8] B. BUDIANSKY and R. J. VIDENSEK, Analysis of stresses in the plastic range around a circular hole in a plate subjected to uniaxial tension. *National Advisory Committee for Aeronautics*, Technical Note No. 3542.
[9] W. RAMBERG and W. R. OSGOOD, Description of stress–strain curves by three parameters. *National Advisory Committee for Aeronautics*, Technical Note No. 902.
[10] G. G. GRIFFITH, Experimental investigation of the effects of plastic flow in a tension panel with a circular hole. *National Advisory Committee for Aeronautics*, Technical Note No. 1705.
[11] A. W. BOX, The effect of plastic strains on stress concentrators. *Proc. Soc. exp. Stress Analysis* **8**, 99 (1951).
[12] J. R. DIXON, Elastic–plastic strain distribution in flat bars containing holes or notches. *J. Mech. Phys. Solids* **10**, 253 (1962).
[13] A. J. DURELLI and C. A. SCIAMMARELLA, Elastoplastic stress and strain distribution in a finite plate with a circular hole subjected to undimensional load. *J. appl. Mech.* **30** E, 115 (1963).
[14] B. FRIED and N. H. SHOUP, A study in photoplasticity: the photoelastic effect in the region of large deformation in polyethylene. *Proc. 2nd U.S. Natn. Congr. Applied Mechanics*, Ann Arbor, Michigan, 1954.
[15] M. M. FROCHT and R. A. THOMSON, Studies in photoplasticity. *Proc. 3rd U.S. Natn. Congr. Applied Mechanics*, pp. 533–540, 1958.
[16] R. E. PETERSON, Fatigue of metals in engineering and design. Edgar Marberg Lecture of SESA, 1962.

APPENDIX A

EXPANSIONS OF THE GOVERNING EQUATION

1. *Arbitrary three dimensional orthogonal curvilinear coordinate system*

The equilibrium equation for coordinate direction x_1 is

$$
\begin{aligned}
& C_{1;11}\frac{\partial^2 u_1}{\partial x_1^2}+C_{1;22}\frac{\partial^2 u_1}{\partial x_2^2}+C_{1;33}\frac{\partial^2 u_1}{\partial x_3^2}+C_{1;1}\frac{\partial u_1}{\partial x_1}+C_{1;2}\frac{\partial u_1}{\partial x_2}+C_{1;3}\frac{\partial u_1}{\partial x_3}+C_1 u_1 \\
&\quad +C_{2;12}\frac{\partial^2 u_2}{\partial x_1 \partial x_2}+C_{2;1}\frac{\partial u_2}{\partial x_1}+C_{2;2}\frac{\partial u_2}{\partial x_2}+C_2 u_2+C_{3;13}\frac{\partial^2 u_3}{\partial x_1 \partial x_3} \\
&\quad +C_{3;1}\frac{\partial u_3}{\partial x_1}+C_{3;3}\frac{\partial u_3}{\partial x_3}+C_3 u_3 \\
&= C_{11;1}\frac{\partial \epsilon''_{11}}{\partial x_1}+C_{22;1}\frac{\partial \epsilon''_{22}}{\partial x_1}+C_{12;2}\frac{\partial \gamma''_{12}}{\partial x_2}+C_{13;3}\frac{\partial \gamma''_{13}}{\partial x_3} \\
&\quad +C_{11}\epsilon''_{11}+C_{22}\epsilon''_{22}+C_{33}\epsilon''_{33}+C_{12}\gamma''_{12}+C_{13}\gamma''_{13} \qquad \text{(A1)}
\end{aligned}
$$

where

$$C_{1;11} = (\lambda+2\mu)\frac{h_2 h_3}{h_1} \qquad \text{(A2a)}$$

$$C_{1;22} = \mu\frac{h_1 h_3}{h_2} \qquad \text{(A2b)}$$

$$C_{1;33} = \mu\frac{h_1 h_2}{h_3} \qquad \text{(A2c)}$$

$$C_{1;1} = (\lambda+2\mu)\left(-\frac{h_2h_3}{h_1^2}\frac{\partial h_1}{\partial x_1}+\frac{h_3}{h_1}\frac{\partial h_2}{\partial x_1}+\frac{h_2}{h_1}\frac{\partial h_3}{\partial x_1}\right) \tag{A2d}$$

$$C_{1;2} = \mu\left(-\frac{h_1h_3}{h_2^2}\frac{\partial h_2}{\partial x_2}+\frac{h_3}{h_2}\frac{\partial h_1}{\partial x_2}+\frac{h_1}{h_2}\frac{\partial h_3}{\partial x_2}\right) \tag{A2e}$$

$$C_{1;3} = \mu\left(-\frac{h_1h_2}{h_3^2}\frac{\partial h_3}{\partial x_3}+\frac{h_1}{h_3}\frac{\partial h_2}{\partial x_3}+\frac{h_2}{h_3}\frac{\partial h_1}{\partial x_3}\right) \tag{A2f}$$

$$\begin{aligned} C_1 = {} & \lambda\left[\frac{h_3}{h_1}\frac{\partial^2 h_2}{\partial x_1^2}+\frac{h_2}{h_1}\frac{\partial^2 h_3}{\partial x_1^2}\right]-\mu\left[\frac{h_2}{h_3}\frac{\partial^2 h_1}{\partial x_3^2}+\frac{h_3}{h_2}\frac{\partial^2 h_1}{\partial x_2^2}+\frac{h_3}{h_1h_2}\left(\frac{\partial h_1}{\partial x_2}\right)^2+\frac{h_2}{h_1h_3}\left(\frac{\partial h_1}{\partial x_3}\right)^2\right. \\ & \left.+\frac{1}{h_2}\frac{\partial h_1}{\partial x_2}\frac{\partial h_3}{\partial x_2}+\frac{1}{h_3}\cdot\frac{\partial h_1}{\partial x_3}\frac{\partial h_2}{\partial x_3}-\frac{h_2}{h_3^2}\frac{\partial h_1}{\partial x_3}\frac{\partial h_3}{\partial x_3}-\frac{h_3}{h_2^2}\frac{\partial h_1}{\partial x_2}\frac{\partial h_2}{\partial x_2}\right] \\ & -\lambda\left[\frac{h_3}{h_1^2}\frac{\partial h_1}{\partial x_1}\frac{\partial h_2}{\partial x_1}+\frac{h_2}{h_1^2}\frac{\partial h_1}{\partial x_1}\frac{\partial h_3}{\partial x_1}\right]-(\lambda+2\mu)\left[\frac{h_3}{h_1h_2}\left(\frac{\partial h_2}{\partial x_1}\right)^2+\frac{h_2}{h_1h_3}\left(\frac{\partial h_3}{\partial x_1}\right)^2\right] \end{aligned} \tag{A2g}$$

$$C_{2;12} = (\lambda+\mu)h_3 \tag{A2h}$$

$$C_{2;1} = (\lambda+3\mu)\frac{h_3}{h_1}\frac{\partial h_1}{\partial x_2}+(\lambda+\mu)\frac{\partial h_3}{\partial x_2} \tag{A2i}$$

$$C_{2;2} = -(\lambda+3\mu)\frac{h_3}{h_2}\cdot\frac{\partial h_2}{\partial x_1} \tag{A2j}$$

$$\begin{aligned} C_2 = {} & (\lambda+2\mu)\left[\frac{h_3}{h_1}\frac{\partial^2 h_1}{\partial x_1\partial x_2}-\frac{h_3}{h_1^2}\frac{\partial h_1}{\partial x_1}\frac{\partial h_1}{\partial x_2}-\frac{1}{h_3}\frac{\partial h_3}{\partial x_1}\frac{\partial h_3}{\partial x_2}\right] \\ & -(\lambda+\mu)\left[\frac{h_3}{h_1h_2}\frac{\partial h_1}{\partial x_2}\frac{\partial h_2}{\partial x_1}+\frac{1}{h_2}\frac{\partial h_2}{\partial x_1}\frac{\partial h_3}{\partial x_2}\right]+\lambda\frac{\partial^2 h_3}{\partial x_1\partial x_2} \\ & +\mu\left[\frac{h_3}{h_2^2}\frac{\partial h_2}{\partial x_1}\frac{\partial h_2}{\partial x_2}-\frac{h_3}{h_2}\frac{\partial^2 h_2}{\partial x_1\partial x_2}+\frac{2}{h_1}\frac{\partial h_1}{\partial x_2}\frac{\partial h_3}{\partial x_1}\right] \end{aligned} \tag{A2k}$$

$$C_{3;13} = (\lambda+\mu)h_2 \tag{A2l}$$

$$C_{3;1} = (\lambda+3\mu)\frac{h_2}{h_1}\frac{\partial h_1}{\partial x_3}+(\lambda+\mu)\frac{\partial h_2}{\partial x_3} \tag{A2m}$$

$$C_{3;3} = -(\lambda+3\mu)\frac{h_2}{h_3}\frac{\partial h_3}{\partial x_1} \tag{A2n}$$

$$\begin{aligned} C_3 = {} & (\lambda+2\mu)\left[\frac{h_2}{h_1}\frac{\partial^2 h_1}{\partial x_1\partial x_3}-\frac{h_2}{h_1^2}\frac{\partial h_1}{\partial x_1}\frac{\partial h_1}{\partial x_3}-\frac{1}{h_2}\frac{\partial h_2}{\partial x_1}\frac{\partial h_2}{\partial x_3}\right] \\ & -(\lambda+\mu)\left[\frac{h_2}{h_1h_3}\frac{\partial h_1}{\partial x_3}\frac{\partial h_3}{\partial x_1}+\frac{1}{h_3}\frac{\partial h_3}{\partial x_1}\frac{\partial h_2}{\partial x_3}\right]+\lambda\frac{\partial^2 h_2}{\partial x_1\partial x_3} \\ & +\mu\left[\frac{h_2}{h_3^2}\frac{\partial h_3}{\partial x_1}\frac{\partial h_3}{\partial x_3}-\frac{h_2}{h_3}\frac{\partial^2 h_3}{\partial x_1\partial x_3}+\frac{2}{h_1}\frac{\partial h_1}{\partial x_3}\frac{\partial h_2}{\partial x_1}\right] \end{aligned} \tag{A2o}$$

$$C_{11;1} = 2\mu h_2h_3 \tag{A2p}$$

$$C_{12;2} = \mu h_1 h_3 \tag{A2q}$$

$$C_{13;3} = \mu h_1 h_2 \tag{A2r}$$

$$C_{11} = 2\mu\left(h_2\frac{\partial h_3}{\partial x_1} + h_3\frac{\partial h_2}{\partial x_1}\right) \tag{A2s}$$

$$C_{22} = -2\mu h_3\frac{\partial h_2}{\partial x_1} \tag{A2t}$$

$$C_{33} = -2\mu h_2\frac{\partial h_3}{\partial x_1} \tag{A2u}$$

$$C_{12} = \mu\left(h_1\frac{\partial h_3}{\partial x_2} + 2h_3\frac{\partial h_1}{\partial x_2}\right) \tag{A2v}$$

$$C_{13} = \mu\left(h_1\frac{\partial h_2}{\partial x_3} + 2h_2\frac{\partial h_1}{\partial x_3}\right) \tag{A2w}$$

$$C_{22;1} = 0 \tag{A2x}$$

The corresponding equations for the other coordinate directions can be obtained by cyclic rotation of the subscripts 1, 2, 3.

2. *Plane strain*

The above equations also hold for two dimensional plane strain conditions. In that case

$$u_3 = 0, \qquad h_3 = 1$$

and furthermore all derivatives with respect to x_3 are zero.

3. *Plane stress*

For plane stress conditions the coefficients in equation (A1) take the forms:

$$C_{1;11} = \frac{h_2}{h_1} \tag{A3a}$$

$$C_{1;22} = \frac{1-\nu}{2}\frac{h_1}{h_2} \tag{A3b}$$

$$C_{1;1} = \frac{1}{h_1}\left(\frac{\partial h_2}{\partial x_1} - \frac{h_2}{h_1}\frac{\partial h_1}{\partial x_1}\right) \tag{A3c}$$

$$C_{1;2} = \frac{1-\nu}{2}\cdot\frac{1}{h_2}\left(\frac{\partial h_1}{\partial x_2} - \frac{h_1}{h_2}\frac{\partial h_2}{\partial x_2}\right) \tag{A3d}$$

$$\begin{aligned} C_1 = {} & \frac{\nu}{h_1}\left(\frac{\partial^2 h_2}{\partial x_1^2} - \frac{1}{h_1}\frac{\partial h_1}{\partial x_1}\frac{\partial h_2}{\partial x_1}\right) - \frac{1}{h_1 h_2}\left(\frac{\partial h_2}{\partial x_1}\right)^2 \\ & + \frac{1-\nu}{2}\left[\frac{-1}{h_1 h_2}\left(\frac{\partial h_1}{\partial x_2}\right)^2 + \frac{1}{h_2^2}\frac{\partial h_2}{\partial x_2}\frac{\partial h_1}{\partial x_2} - \frac{1}{h_2}\cdot\frac{\partial^2 h_1}{\partial x_2^2}\right] \end{aligned} \tag{A3e}$$

$$C_{2;12} = \frac{1+\nu}{2} \tag{A3f}$$

$$C_{2;1} = \frac{3-\nu}{2}\cdot\frac{1}{h_1}\frac{\partial h_1}{\partial x_2}+\frac{1-\nu}{h_2}\frac{\partial h_2}{\partial x_2} \tag{A3g}$$

$$C_{2;2} = -\frac{3-\nu}{2}\frac{1}{h_2}\frac{\partial h_2}{\partial x_1} \tag{A3h}$$

$$C_2 = \frac{1}{h_1}\frac{\partial^2 h_1}{\partial x_1 \partial x_2} - \frac{1}{h_1^2}\frac{\partial h_1}{\partial x_1}\frac{\partial h_1}{\partial x_2} + \frac{1-\nu}{2}\left(\frac{1}{h_2^2}\frac{\partial h_2}{\partial x_1}\frac{\partial h_2}{\partial x_2} - \frac{1}{h_2}\frac{\partial^2 h_2}{\partial x_1 \partial x_2}\right) - \frac{1+\nu}{2}\frac{1}{h_1 h_2}\frac{\partial h_2}{\partial x_1}\frac{\partial h_1}{\partial x_2} \tag{A3i}$$

$$C_{11;1} = h_2 \tag{A3j}$$

$$C_{12;2} = \frac{1-\nu}{2}h_1 \tag{A3k}$$

$$C_{11} = (1-\nu)\frac{\partial h_2}{\partial x_1} \tag{A3l}$$

$$C_{22} = -(1-\nu)\frac{\partial h_2}{\partial x_1} \tag{A3m}$$

$$C_{12} = (1-\nu)\frac{\partial h_1}{\partial x_2} \tag{A3n}$$

$$C_{22;1} = \nu\,.\,h_2 \tag{A3o}$$

All other coefficients are zero.

APPENDIX B

DESCRIPTION OF A NUMERICAL METHOD OF SOLUTION

Due to symmetry only one-fourth of the actual region needs to be considered. This quarter is divided into curvilinear network of squares, as shown on Fig. B1. The angle $\mathrm{d}\theta$ is $\pi/2N$, so that $\theta_n = n\pi/2N$. From geometrical relations the radius can be expressed as $r_m = \xi^{m-1}a$, where $\xi = (2+\mathrm{d}\theta)/(2-\mathrm{d}\theta)$. Similarly $\mathrm{d}r_m = (\xi-1)\xi^{m-2}a$. The derivatives of some function ϕ at radius r_m with respect to r can be obtained as

$$\left.\frac{\mathrm{d}\phi}{\mathrm{d}r}\right|_m = \frac{1}{r_m}\left[\varkappa_1\phi_{m+1}+\phi_m-\varkappa_2\phi_{m-1}\right] \tag{B1a}$$

$$\left.\frac{\mathrm{d}^2\phi}{\mathrm{d}r^2}\right|_m = \frac{1}{r_m^2}\left[\varkappa_3\phi_{m+1}-\varkappa_4\phi_m+\varkappa_5\phi_{m-1}\right] \tag{B1b}$$

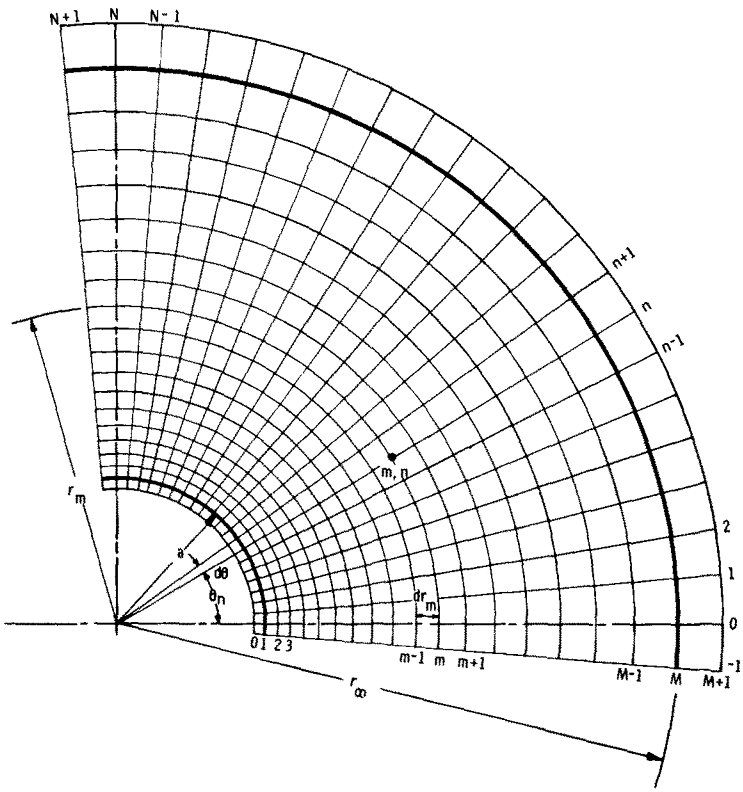

FIG. B1. Illustration for the numerical solution.

where the $\varkappa - s$ are constants

$$\left.\begin{aligned} \varkappa_1 &= \frac{1}{\xi^2-1}; \qquad \varkappa_2 = \frac{\xi^2}{\xi^2-1}; \qquad \varkappa_3 = \frac{2\xi}{(\xi-1)^2(\xi+1)}; \\ \varkappa_4 &= \frac{2\xi}{(\xi-1)^2}; \qquad \varkappa_5 = \frac{2\xi^2}{(\xi-1)^2(\xi+1)}. \end{aligned}\right\} \tag{B2}$$

Derivatives with respect to θ can be written as

$$\left.\frac{d\phi}{d\theta}\right|_n = \varkappa_6(\phi_{n+1}-\phi_{n-1}) \tag{B3a}$$

$$\left.\frac{d^2\phi}{d\theta^2}\right|_n = \varkappa_7(\phi_{n+1}-2\phi_n+\phi_{n-1}) \tag{B3b}$$

where

$$\varkappa_6 = \frac{1}{2d\theta}; \qquad \varkappa_7 = \frac{1}{d\theta^2}. \tag{B4}$$

Define the following constants for convenience

$$
\left.
\begin{aligned}
&b_1 = \varkappa_1+\varkappa_2 && b_8 = 2-\nu && b_{15} = \frac{1-\nu}{2}(\varkappa_5-\varkappa_2)\\
&b_2 = -\varkappa_4-(1-\nu)\varkappa_7 && b_9 = 2\nu-1 && b_{16} = 2\varkappa_6\\
&b_3 = \varkappa_5-\varkappa_2 && b_{10} = \nu\varkappa_1 && b_{17} = \nu\varkappa_6\\
&b_4 = \frac{1-\nu}{2}\varkappa_6 && b_{11} = -\nu\varkappa_2 && b_{18} = \frac{1-\nu}{2}\varkappa_1\\
&b_5 = (1-\nu)\varkappa_6 && b_{12} = \frac{1-\nu}{2}\varkappa_6 && b_{19} = -\frac{1-\nu}{2}\varkappa_2\\
&b_6 = \frac{1+\nu}{2}\varkappa_1\varkappa_6 && b_{13} = \frac{1-\nu}{2}(\varkappa_1+\varkappa_3) && b_{20} = \tfrac{3}{2}(1-\nu)\\
&b_7 = \frac{1+\nu}{2}\varkappa_2\varkappa_6 && b_{14} = -\frac{1-\nu}{2}\varkappa_4-2\varkappa_7 &&
\end{aligned}
\right\} \quad \text{(B5)}
$$

At any stage of the computations, when the displacements u,v and the plastic strain components ϵ_r'', ϵ_θ'', $\gamma_{r\theta}''$, are substituted into the governing equations, they will not be satisfied identically. The error at the point (m, n) in finite difference form can be written as

$$
\begin{aligned}
R_{u_{m,n}} = {} & \frac{1}{r_m^2}\Big[b_1u_{m+1,n}+b_2u_{m,n}+b_3u_{m-1,n}+b_4(u_{m,n+1}+u_{m,n-1})+b_5(v_{m,n-1}-v_{m,n+1})\\
& +b_6(v_{m+1,n+1}-v_{m+1,n-1})+b_7(v_{m-1,n-1}-v_{m-1,n+1})\Big]\\
& -\frac{1}{r_m}\Big[\varkappa_1\epsilon''_{r_{m+1,n}}+b_8\epsilon''_{r_{m,n}}-\varkappa_2\epsilon''_{r_{m-1,n}}+b_{10}\epsilon''_{\theta_{m+1,n}}\\
& +b_9\epsilon''_{\theta_{m,n}}+b_{11}\epsilon''_{\theta_{m-1,n}}+b_{12}(\gamma''_{r\theta_{m,n+1}}-\gamma''_{r\theta_{m,n-1}})\Big].
\end{aligned} \quad \text{(B6a)}
$$

$$
\begin{aligned}
R_{v_{m,n}} = {} & \frac{1}{r_m^2}\Big[b_{13}v_{m+1,n}+b_{14}v_{m,n}+b_{15}v_{m-1,n}+\varkappa_7(v_{m,n+1}+v_{m,n-1})+b_{16}(u_{m,n+1}-u_{m,n-1})\\
& +b_6(u_{m+1,n+1}-u_{m+1,n-1})+b_7(u_{m-1,n-1}-u_{m-1,n+1})\Big]\\
& -\frac{1}{r_m}\Big[b_{17}(\epsilon''_{r_{m,n+1}}-\epsilon''_{r_{m,n-1}})+\varkappa_6(\epsilon''_{\theta_{m,n+1}}-\epsilon''_{\theta_{m,n-1}})\\
& +b_{18}\gamma''_{r\theta_{m+1,n}}+b_{19}\gamma''_{r\theta_{m-1,n}}+b_{20}\gamma''_{r\theta_{m,n}}\Big].
\end{aligned} \quad \text{(B6b)}
$$

Note that subscripts here denote locations as shown on Fig. B1. After these preliminaries the numerical solutions can be outlined as follows.

First, the known elastic solution [4] is used. The displacements are calculated for every point (m, n) and the plastic strains are set equal to zero. Thus equations (14) are satisfied identically. When the displacements of the exact elastic solution are substituted into the equations (B6) small residuals are obtained because of the finite difference representation of the differential equations. Name these residuals $R^*_{u_{m,n}}$ and $R^*_{v_{m,n}}$. Later in the computations these residuals will serve as limits of convergence.

Based on the elastic solution the plastic strains are estimated. This process is described in [1–3] in detail and only a brief review is given here for the deformation theory. From the uniaxial stress–strain curve an effective total strain, effective plastic strain relation is deduced. The instantaneous effective total strain is assumed to be correct and the corresponding effective plastic strain is computed from the known relation between them. Denote their ratio as $\psi_{m,n} = \epsilon''_{\text{eff}_{m,n}}/\epsilon_{\text{eff}_{m,n}}$. The estimates for the plastic strains will now be

$$\epsilon''_{r_{m,n}} = \tfrac{1}{3}\psi_{m,n}(2\epsilon_r - \epsilon_\theta - \epsilon_z)_{m,n}, \tag{B7a}$$

$$\epsilon''_{\theta_{m,n}} = \tfrac{1}{3}\psi_{m,n}(2\epsilon_\theta - \epsilon_r - \epsilon_z)_{m,n}, \tag{B7b}$$

$$\gamma''_{r\theta_{m,n}} = \psi_{m,n}\gamma_{r\theta_{m,n}}, \tag{B7c}$$

and due to the incompressibility of the plastic part of the material

$$\epsilon''_{z_{m,n}} = -(\epsilon''_r + \epsilon''_\theta)_{m,n} \tag{B7d}$$

Of course at the start the plastic strains will be different from zero only where the effective stress of the elastic solution is larger than σ_Y.

Next the estimated plastic strain components are substituted into equations (B6) which now have to be solved for the displacements u and v, so that the residuals R_u and R_v will be lower or equal to R_u^* and R_v^*, furthermore the appropriate boundary conditions will be satisfied.

Some questions may arise concerning how the various derivatives of the plastic strain can be evaluated at the neighborhood of the instantaneous elastic–plastic boundary. It was found that for stress–strain curves of the type which are shown on Fig. 2 the transition from elastic to elastic–plastic region is very smooth, therefore, no special considerations are needed; equations (B6) can be used without modifications. When bilinear stress–strain curves are used with very low strain hardening, the change is quite abrupt and the use of appropriate forward or backward finite difference equations is advisable.

For the estimated plastic strain distribution equations (B6) are solved for u and v by a simultaneous over-relaxation method. When operating on (B6a) the displacements v are fixed and displacements u are replaced

$$u_{m,n}^{\text{new}} = u_{m,n}^{\text{old}} - \frac{\omega R_{u_{m,n}} r_m^2}{b_2} \tag{B8a}$$

where ω is an over-relaxation factor obtained by trial and error. When operating on (B6b) the displacements u are fixed and v are replaced

$$v_{m,n}^{\text{new}} = v_{m,n}^{\text{old}} - \frac{\omega R_{v_{m,n}} r_m^2}{b_{14}} \tag{B8b}$$

Which of the two equations to operate on is decided on the basis of the maximum relative deviation of R_u from R_u^* and R_v from R_v^*.

In numerical solutions infinite regions cannot be really achieved. Instead an outer boundary with a large radius, r_∞, is used. On this boundary the radial and shear stresses are maintained the same as given by the elastic solution, and this distribution is considered as an external load.

Instead of using special forward and backward operators at the boundaries, it is convenient to use some fictitious points outside of the actual region and set the values at these points of the displacements always so, that the boundary conditions be satisfied at any time.

Once equations (B6) are satisfied, a first approximation for the elastic–plastic problem is known. The results however are not correct as yet and must be improved by computing new plastic strain components on the basis of the latest effective total strains. During this process not only the magnitudes of the plastic strains change but also the boundaries of the plastic region, since certain points may move in or out of the instantaneous plastic region. For the new plastic strains, equations (B6) are resolved again.

This process must be followed until the effective stresses and effective total strains fall on or sufficiently close to the effective stress, effective strain curve.

The number of loops required depends mainly on the shape of the stress–strain curve, and the degree of loading. In the examples given in the paper an average of twenty loops gave sufficiently accurate answers.

In order to establish the effect of mesh size on the results, the most sensitive strain concentration factors were plotted against variable mesh sizes used. It was found that the factor is increasing for increasing number of mesh points but it also levels off and the limiting value is quite easily predictable. The examples presented are on the basis of $M = 30$, $N = 20$ ($r_\infty = 9{\cdot}765$). In most cases the computed and the predicted limiting concentration factors are within a fraction of one percent. At the highest loads the deviation is in the order of one per cent.

(*Received* 15 *December* 1965; *revised* 31 *May* 1966)

Résumé—Le problème général élastique–plastique à trois dimensions est formulé en termes des déplacements totaux et des composantes de déformation plastique. Les équations gouvernantes résultant sont applicable à des systèmes arbitraires orthogonaux curvilinéaires coordinés et à des théories arbitraires de plasticité. Une méthode a été développée pour la solution de deux problèmes dimensionnels et est employée pour l'analyse d'un trou circulaire dans une plaque plate sous une tension uniaxiale. La même méthode pourrait être généralisée pour trois dimensions.

L'objet du rapport est d'illustrer qu'une approche simple et directe peut être employée pour formuler et résoudre des problèmes élastiques plastiques autrement très compliqués et non résolus pour la plupart.

Zusammenfassung—Das allgemeine dreidimensionale elastisch–plastische Problem wird durch Totalverschiebungen und durch plastische Verzerrungskomponenten ausgedrückt. Die resultierenden Gleichungen können angewendet werden in willkürlichen, orthogonalen, krummlinigen Koordinatensystemen sowie in willkürlichen Theorien der Plastizität. Eine Methode für die Lösung zweidimensionaler Probleme wird entwickelt und zur Analyse einer ringförmigen Öffnung in einer flachen Platte bei einachsiger Spannung angewendet.

Dieselbe Methode könnte auch für drei Dimensionen verallgemeinert werden.

Es ist der Zweck der Arbeit eine einfache und direkte Methode zu finden um elastisch–plastische Probleme, die sonst sehr kompliziert und oft ungelöst sind entsprechend zu formulieren und zu lösen.

Абстракт—Общая трёхмерная упруго–пластическая проблема формулируется с точки зрения полных смещений и составных частей пластической деформации. Получающиеся в результате управляющие уравнения применимы для систем произвольной ортогонаьной криволинейной координаты и в произвольных теориях пластичности. Разработан метод для решения двумерных проблем, который применяется для анализа кругового отверстия в плоской пластине под одноосным напряжением. Этот же самый метод может быть обобщён для трёх размерностей.

Цель статьи- пояснить то, что непосредственный простой подход может применятьсн для формулировки и решения очень сложных и в большинстве случаев иным способом неразрешимых пластических проблем.